TESTING OF A COLLET CHUCK IN THE STABILIZATION OF THE TURNING PROCESS

DANIEL KUCERKA[1], MICHAELA MAJERNIKOVA[2], JIRI DOSTAL[1], JAN MAJERNIK[3,4], KAREK SRAMHAUSER[3], PAVEL CERNY[3,5], MICHAL MRAZEK[1]

[1]Department of Technical Education and Information Technology, Faculty of Education, Palacky University Olomouc, Olomouc, Czech Republic

[2]Department of Machining and Assembly, Faculty of Mechanical Engineering, Technical University of Liberec, Liberec, Czech Republic

[3]Department of Technology and Cybernetics, Faculty of Agriculture and Technology, University of South Bohemia in Ceske Budejovice, Ceske Budejovice. Czech Republic

[4]Department of Mechanical Engineering, Faculty of Technology, The Institute of Technology and Business in Ceske Budejovice, Ceske Budejovice. Czech Republic

[5]Department of Physics, Technology and Chemistry, Faculty of Education, University of South Bohemia in Ceske Budejovice, Ceske Budejovice. Czech Republic

DOI: 10.17973/MMSJ.2026_11_2026044

jmajernik@jcu.cz

Surface roughness is one of the main quality indicators and often a technical requirement specified for mechanical components, where achieving the proper surface quality is crucial for part functionality. In actual machining, surface roughness is influenced by numerous factors, including cutting parameters, tool variables, and workpiece variables. One of the key factors affecting surface roughness and compliance with specified geometric tolerances is workpiece clamping rigidity. This study evaluates the quality of the machined surface depending on the clamping method of the blank. Surface roughness is compared for components clamped in a universal three-jaw chuck versus a collet chuck, utilizing two types of indexable rhombic cutting inserts: VCGT and VCMT types. The obtained results demonstrate that using a collet chuck stabilizes the cutting process and improves the uniformity of the surface roughness profile of the machined parts.

KEYWORDS

machining process, turning, cutting conditions, collet chuck, surface roughness

1 INTRODUCTION

Given the demand for manufacturing high-precision components with superior dimensional accuracy and surface quality, machining processes represent the foundation of the manufacturing sector [Mane 2025a]. Turning is one of the most widely used and essential technologies in the precision machining of steel parts due to its high efficiency. Provided that surface texture characteristics allow, grinding can be replaced by turning, as comparable precision and surface quality can be achieved, eliminating the need for subsequent finishing operations [Mathivanan 2021, Molnar 2023]. Driven by productivity and efficiency, CNC lathes have gained widespread popularity, offering numerous advantages such as operational flexibility and a high degree of automation [Dua 2025, Sorbino 2025].

In today's manufacturing industry, the demand for high-precision, high-productivity, and synchronized production is rapidly growing. This trend is driven by the widespread implementation of CNC technologies, automation systems, and mass production lines, which place greater emphasis on the role of auxiliary manufacturing tools, particularly workholding and fixture systems [Bratan 2023, Coranic 2023]. Consequently, fixtures have become indispensable and increasingly specialized to address the evolving challenges in modern machining applications [Anh 2025, Qin 2025].

In scenarios where high-performance machining methods are increasingly adopted, the auxiliary time required for workpiece clamping becomes disproportionately high relative to the actual machine operating time. Under such conditions, productivity can be enhanced not only by optimizing cutting parameters, but also by employing specialized tooling or dedicated chucking systems that yield reduced clamping times and higher precision [Botak 2024, Mituriska 2020]. One strategy to improve the productivity of automated processing is using a relatively large workpiece overhang, which minimizes non-productive auxiliary time and enhances the continuity of the manufacturing cycle. However, increasing spindle speed—a primary reserve for driving productivity—complicates the dynamic behavior of the "spindle–workpiece–tool" system when processing long blanks with extended overhangs [Cubonova 2019]. Unlike conventional short and relatively rigid workpieces, an unsupported long workpiece exhibits increased flexural compliance; consequently, its rotation may give rise to elevated deflections, eccentricity, and transverse vibrations driven by its self-weight, initial unbalance, clamping compliance, spindle support stiffness, and clamping conditions [Olejarova 2021, Urgas 2025, Prydalnyj 2026]. In addition to the aforementioned adverse effects during turning, high cutting forces generated when machining long unsupported workpieces typically induce static deflections. On the one hand, these deflections compromise machining accuracy, leading to high scrap rates or labor-intensive rework with elevated unit costs. On the other hand, insufficient dynamic stiffness of the workpiece–fixture system often triggers unwanted regenerative chatter, which degrades surface quality, leaves chatter marks, and can even damage or destroy the components [Feng 2022, Feng 2025].

Modulating surface quality and production efficiency can also be achieved by increasing spindle speed, and consequently, cutting speed [Hrehova 2016]. However, operating speeds approaching the natural frequency of such a system induce resonance-hazardous and destructive operating regimes. Under these conditions, radial runout of the bar stock increases, maintaining a stable workpiece position within the machining zone becomes more challenging, conditions for achieving dimensional accuracy and surface quality deteriorate, and dynamic loads on the spindle assembly components and its supports increase. Consequently, potential productivity gains achieved through higher speeds are constrained not only by drive power or structural component strength, but also by the vibrational stability of the bar stock system. In practice, this necessitates identifying speed regimes prior to cutting where the rotation of a long bar stock workpiece does not trigger unsafe vibration amplification. In this respect, determining the effect of bar diameter, distance between clamping and support points, and support stiffness on the critical speed is of paramount importance [Otto 2015, Sakamoto 2012].

The negative aspects resulting from inadequate stiffness of the spindle–chuck–workpiece system are further amplified when machining hard materials under extended workpiece overhang.

One category of materials with demanding machining requirements is austenitic stainless steels. Compared to other steels, machining austenitic stainless steels is more challenging due to their high tensile strength, high ductility, high work hardening rate, low thermal conductivity, and strong tendency toward built-up edge (BUE) formation. Austenitic stainless steel AISI 304 is an alloy with strategic properties, such as good corrosion resistance, good formability, and non-magnetic characteristics. These properties qualify this steel grade as a well-suited choice for numerous applications across various sectors, including the marine, chemical and petroleum, food processing, and nuclear power industries [Boucherit 2021, Zhang 2022]. High-speed machining of stainless steel has long been a subject of research. Due to its inherent properties (low thermal conductivity and work-hardening tendency), AISI 304 steel is classified as a difficult-to-cut material. Tool life and the quality of the machined surface represent two of the most critical indicators of machining process efficiency and overall performance [Chinchanikar 2023].

Enhancing machining accuracy and maintaining the specified surface quality characteristics of final components can be achieved through the implementation of collet chucks. Collet chucks are actuated by two primary mechanisms: push-type or pull-type. The operating principle of collet chucks is based on the wedge effect, as illustrated in Fig. 1. The axial movement of the collet (2) or taper (4) causes the contraction or expansion of the collet segments, thereby generating the clamping motion. Furthermore, the applied axial force increases the normal force acting on the collet, which in turn increases the frictional force and the maximum transmissible torque [Heras 2020].

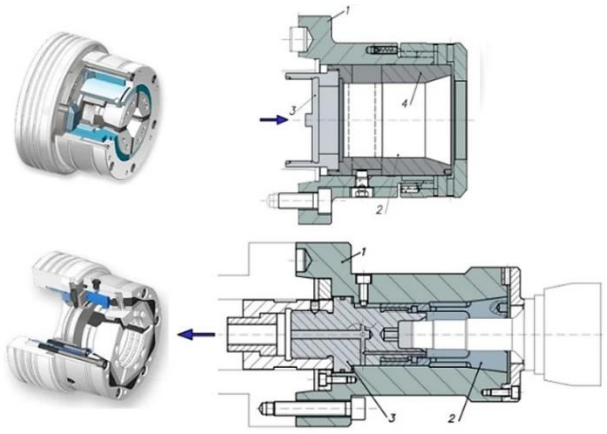


Figure 1. Collet chuck acting by pushing and by pulling [Heras 2020]

In this study, the authors investigate the potential to increase machining productivity using a collet chuck. During several experimental works focusing on the machining of austenitic steels conducted by the research team (e.g., [Sorbino 2025]), it was observed that the surface roughness of components manufactured with a relatively large overhang without tailstock support exhibits high scatter. This variation depends both on the distance of the evaluated location from the chuck and on the setting of cutting conditions and the type of indexable insert used. In high-volume repetitive production, the auxiliary time required to support the blank with a live center in the tailstock represents non-productive time that slows down overall throughput. This study evaluates manufacturing quality by assessing the surface roughness of selected components produced using a universal three-jaw chuck compared to clamping in a collet chuck. Based on the obtained results, it is demonstrated that employing a collet chuck enhances workpiece clamping rigidity, contributes to stabilizing the cutting process, and, as confirmed by standard deviation analysis, yields a more uniform surface roughness profile.

2 DESCRIPTION OF EXPERIMENTAL PROCEDURE

The present study builds upon the experiments presented in the publication "SUITABILITY OF VCGT AND VCMT CUTTING INSERTS TYPE FOR TURNING ALSI 304 STEEL" [Sorbino 2025]. Testing of the collet chuck in stabilizing the cutting process and comparing the surface roughness characteristics of the machined components against a universal three-jaw chuck was conducted during the production of components shown in Fig. 2. The component is manufactured from AISI 304 (1.4301) stainless steel using a Ø24 mm round bar as the blank material.

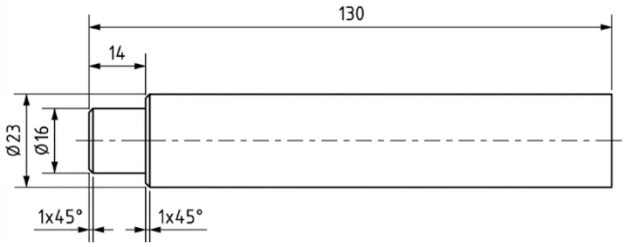


Figure 2. Geometry and dimensions of the turned workpiece

The chemical composition of the base material was verified against the standard specifications using a Bruker Q4 Tasman spark optical emission spectrometer. Table 1 presents the elemental mass percentages of the steel compared with the values specified by the EN 10088-1 standard for AISI 304 steel designated in accordance with EN 10027-2.

Element	Values according to CSN EN 10088-1 (wt %)	Measured value (wt. %)
C	≤ 0.030	0.025
Si	≤ 1.000	0.371
Mn	≤ 2.000	1.696
P	≤ 0.045	0.031
S	≤ 0.015	0.034
Cr	17.500 – 19.500	19.140
Ni	8.000 – 10.500	8.932

Table 1. Chemical composition of the workpiece blank

The components were machined using VCGT and VCMT indexable cutting inserts. The VCGT-type insert, specifically designated as VCGT 110304FN-ASF AM7020, is a coated carbide insert designed for machining stainless steels, titanium, and hardened steels. It is characterized by high thermal stability, resistance to elevated temperatures and flank wear, reliable tool life, and excellent chip evacuation control. The VCMT-type insert, specifically designated as VCMT 110304EN-PMT1 AM5120, is a coated carbide insert intended for rough machining stainless steels and heat-resistant alloys. It features high flank wear resistance, excellent thermal resistance, reliable tool life, and effective chip control. Both cutting inserts are manufactured by ARNO Werkzeuge and were recommended by TMC CR, s.r.o., during manufacturing technology consultations for a new project implementation. The evaluated indexable cutting inserts along with their characteristic dimensions are illustrated in Fig. 3.

The cutting inserts were mounted on a right-hand turning tool holder designated as SVJCR 2020 K11, manufactured by ARNO Werkzeuge. Insert clamping within the holder was executed using the ISO S system, which utilizes a screw-clamping

mechanism. Component manufacturing was performed on a Masturn MT 550i CNC lathe produced by Kovosvit MAS Machine Tools a.s., equipped with a Heidenhain ManualPlus 620 control system. The technical specifications of the machine include a maximum swing over bed of 550 mm and a swing over cross-slide of 350 mm. The distance between centers is 1,500 mm, the maximum allowable workpiece mass is 600 kg, and the maximum spindle speed reaches 3,000 rpm.

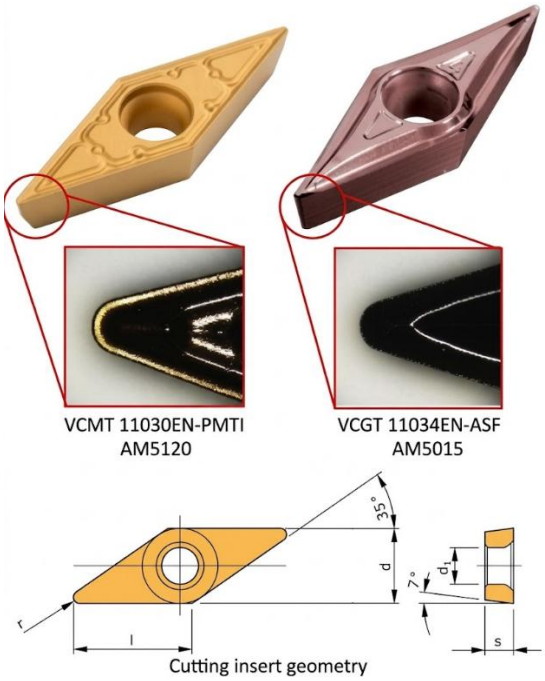


Figure 3. Types of cutting inserts used

The characteristic dimensions of the indexable cutting inserts shown in Fig. 3 are presented in Table 2.

Parameter	VCGT	VCMT
r, (mm)	0.4	0.4
l, (mm)	11.1	11.1
s, (mm)	23.18	23.18
d, (mm)	16.35	16.35
d_1, (mm)	2.9	2.8

Table 2. Geometric parameters of cutting inserts

To evaluate the suitability of using a collet chuck to stabilize the cutting process, four sets of components were manufactured. Two series, corresponding to the respective cutting insert types (VCMT and VCGT), were produced using clamping in a universal three-jaw chuck, while the other two series were produced using clamping in a collet chuck.

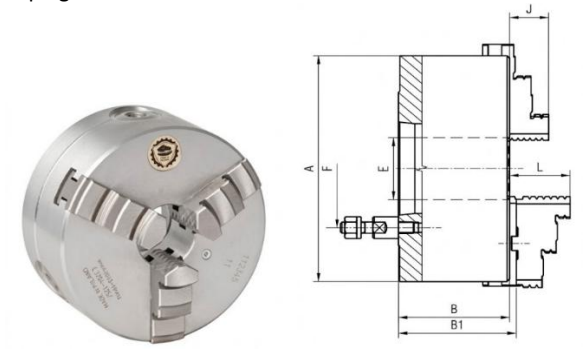


Figure 4. Bison 3534-250-8 universal three-jaw chuck: photograph (left) and schematic drawing (right)

For all series, a constant unsupported overhang length of l = 140 mm from the face of the chuck/collet was maintained. The chuck used is manufactured by Bison and is presented in Fig. 4. The technical specifications of the universal chuck are presented in Table 3.

Parameter	Value	
Product type		3534-250-8
Size	A	250
Number of jaws		3
Jaw type		Solid Jaws
Jaw type		Haer solid jaws
Mounting style		Type C mouting (DIN55027)
Unit of measure		Metric
Taper, KK1 :4		8
RPM n max., 1/min		3500
Accuracy class		Standard
Total length (outside jaws), mm	B	89
Total length (inside jaws), mm	B1	92.8
Thru-hole, mm	E	76
Bolt hole circle, mm	F	171.4
Jaw overhang, mm	J	34
Jaw overhang, mm	L	53
Weight, kg		32
Actuation		Manually actuated

Table 3. Technical specification of the conventional three-jaw chuck

In contrast to a conventional chuck, a collet chuck designated as TOROK RD 65 manufactured by HAINBUCH was tested (see Fig. 5).

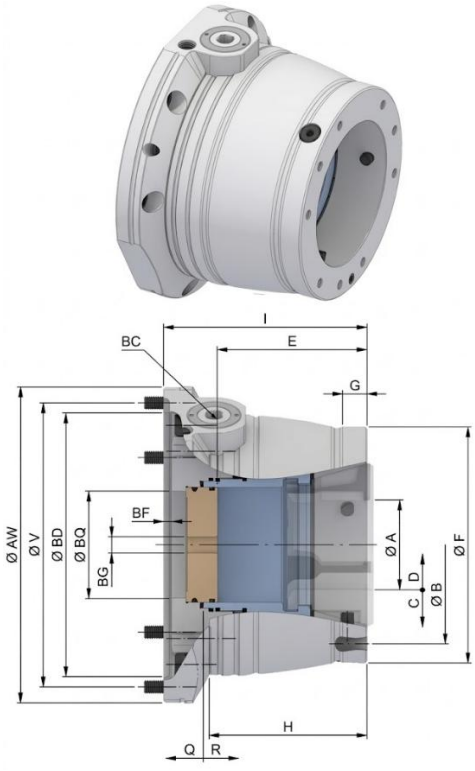


Figure 5. TOROK RD 65

The technical specifications of the collet chuck are presented in Table 4. An SK 65 BZI HSW 24.00 mm rd clamping head was utilized in the chuck.

Parameter	Value	
Product line		RD
Size		65
Run-out ≤, mm		0.010
Max. radial clamping force, kN		105
Max. axial drawtube force [pull / push], kN		45
Flange location	BD	Ø 162 H7
Flange fit length, mm	BF	5.1
Max. actuating torque, Nm	BC	90
RPM n max., 1/min		6000
Clamping range, mm	A	3 - 65
Release stroke in Ø, mm	C	0.6
Reserve stroke in Ø, mm	D	1
Range / recommended workpiece tolerance, mm		± 0.5
End-stop depth, mm	E	92
Ø Capacity, mm	BQ	66
End-stop thread size, mm	BG	12
Location front end-stop	F	Ø 145 f7
Length, mm	H	97
Centering length, mm	G	14
Total length, mm	I	125
Reserve stroke axial, mm	Q	2
Release stroke axia, mm	R	2.5
Bolt hole circle, mm	V	LK Ø 176 [6 x M8]
Outer Ø, mm	AW	194
Weight, kg		14.4
Min. Clamping range, mm		3
Max. Clamping range, mm		65
Actuation		Manually actuated

Table 4. Technical specifications of the collet chuck

The performance of the collet chuck was evaluated with respect to the resulting surface roughness Ra and Rz. Machining tests were conducted under variable cutting conditions according to Table 5. A water-miscible mineral oil emulsion cutting fluid (Blasocut 20) was applied during part production.

Parameter	Value
Cutting depth P, mm	0.5
Cutting speed S, m/min	180
Feed F, mm/rev	0.2

Table 5. Applied cutting parameters

The surface roughness parameters Ra and Rz were measured using a Mitutoyo Surftest SJ-410 device. Surface quality was evaluated in regions A, B, and C (see Fig. 6). At each location, measurements were repeated three times by rotating the component by 120°.

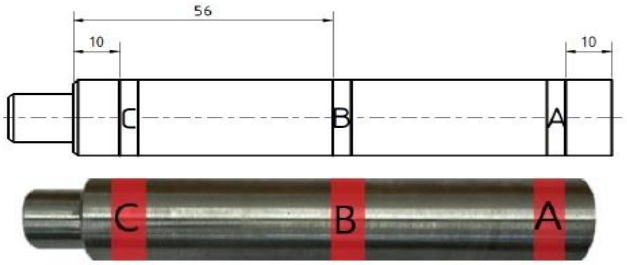


Figure 6. Machined surface roughness Ra/Rz measurement area

The selection of these measurement locations reflects the effect of distance on workpiece deflection caused by clamping without a tailstock center or support. Specifically, this accounts for workpiece radial run-out during unsupported overhang, where surface roughness increases with distance from the chuck toward the free end. Additionally, potential inadequate chip evacuation near the clamping zone was considered.
Table 6 lists the experimental conditions under which the surface roughness parameter Ra of the machined surface was determined.

Parameter	Value
Standard	ISO 1997
Profile	R
Parameter	3
Filter	GAUSS
λc	0.25 mm
λs	2.5 µm
N	5
Pre/Post	On
Delete waves	Off
Profile compensation	Off
Medium Profile	Off

Table 6. Roughness evaluation parameters

3 RESULTS AND DISCUSSION

In each series, twelve workpieces were produced under the cutting conditions specified in Table 5 using cutting fluid. The indexable insert was replaced with a new one after each series. Consequently, result distortion caused by repeated insert usage was avoided. The surface roughness values of the individual evaluated workpieces are presented in the following tables.
Table 7 presents the measured surface roughness Ra values obtained using VCMT indexable inserts under the cutting conditions specified in Table 5 with workpieces clamped in a conventional chuck. The reported Ra values represent the average of three measurements taken at 120° rotations at designated location A, B, or C.

	Mean value Ra, µm		
Sample	Location A	Location B	Location C
1.	1.583	1.797	2.186
2.	1.660	1.694	2.085
3.	1.634	1.703	1.941
4.	1.791	1.789	2.102
5.	1.634	1.806	2.169
6.	1.671	1.785	2.970
7.	1.687	1.733	2.025
8.	1.622	1.728	1.831
9.	1.622	1.716	1.965
10.	1.657	1.751	2.101
11.	1.658	1.729	2.505
12.	1.655	1.726	2.014
Average	1.656	1.746	2.158
Standard deviation	0.048	0.037	0.292

Table 7. Surface roughness Ra for VCMT inserts clamped in a conventional chuck

Table 8 presents the measured surface roughness Rz values obtained using VCMT indexable inserts under the cutting conditions specified in Table 5 with workpieces clamped in a conventional chuck. The reported Rz values represent the

average of three measurements taken at 120° rotations at designated location A, B, or C.

	Mean value Rz, µm		
Sample	Location A	Location B	Location C
1.	8.245	10.124	12.475
2.	8.332	9.347	12.484
3.	8.986	9.854	11.889
4.	9.503	10.374	12.920
5.	8.363	10.229	12.714
6.	9.105	9.826	16.424
7.	8.993	9.494	11.263
8.	8.074	9.408	10.558
9.	8.571	9.080	11.368
10.	10.267	9.526	11.795
11.	7.897	9.003	14.473
12.	8.023	8.843	11.975
Average	8.697	9.592	12.528
Standard deviation	0.671	0.474	1.506

Table 8. Surface roughness Rz for VCMT inserts clamped in a conventional chuck

The measured surface roughness parameters Ra of workpieces clamped in a standard three-jaw chuck and machined with VCGT indexable inserts under the conditions listed in Table 5 are given in Table 9. Each listed Ra value is the mean of three measurements conducted with a 120° rotation at location A, B, or C.

	Mean value Ra, µm		
Sample	Location A	Location B	Location C
1.	1.761	1.819	2.955
2.	1.796	1.877	2.306
3.	1.731	1.867	2.201
4.	1.788	1.899	2.827
5.	1.764	1.879	2.214
6.	1.759	1.855	2.768
7.	1.716	1.896	2.193
8.	1.767	1.883	2.243
9.	1.710	1.841	2.208
10.	1.727	1.886	2.206
11.	1.775	1.951	2.745
12.	1.830	2.041	2.416
Average	1.760	1.891	2.440
Standard deviation	0.034	0.055	0.281

Table 9. Surface roughness Ra for VCGT inserts clamped in a conventional chuck

The measured surface roughness parameters Rz of workpieces clamped in a standard three-jaw chuck and machined with VCGT indexable inserts under the conditions listed in Table 5 are given in Table 10. Each listed Rz value is the mean of three measurements conducted with a 120° rotation at location A, B, or C.

Table 11 presents the measured surface roughness Ra values obtained using VCMT indexable inserts under the cutting conditions specified in Table 5 with workpieces clamped in a collet chuck. The reported Ra values represent the average of three measurements taken at 120° rotations at designated location A, B, or C.

	Mean value Rz, µm		
Sample	Location A	Location B	Location C
1.	8.386	9.495	17.121
2.	10.556	10.217	14.040
3.	8.667	9.936	12.461
4.	8.945	11.670	15.439
5.	8.270	10.160	12.839
6.	8.263	10.577	15.801
7.	8.546	10.535	12.304
8.	8.366	9.511	13.015
9.	8.873	9.993	12.683
10.	8.230	10.203	13.258
11.	9.542	11.543	16.539
12.	10.749	11.839	14.225
Average	8.949	10.473	14.144
Standard deviation	0.843	0.769	1.611

Table 10. Surface roughness Rz for VCGT inserts clamped in a conventional chuck

	Mean value Ra, µm		
Sample	Location A	Location B	Location C
1.	3.059	3.098	3.085
2.	3.098	3.092	3.108
3.	3.085	3.078	3.085
4.	3.050	3.084	3.089
5.	3.038	3.031	3.079
6.	3.052	3.083	2.849
7.	3.085	3.101	3.104
8.	3.080	3.092	3.098
9.	3.068	3.053	3.064
10.	3.174	3.195	3.197
11.	3.147	3.146	3.157
12.	3.299	3.187	3.121
Average	3.103	3.103	3.086
Standard deviation	0.070	0.047	0.080

Table 11. Surface roughness Ra for VCMT inserts clamped in a collet chuck

	Mean value Rz, µm		
Sample	Location A	Location B	Location C
1.	13.382	13.676	13.817
2.	13.154	13.451	13.500
3.	13.301	13.412	13.755
4.	13.131	13.562	13.712
5.	13.258	13.320	13.944
6.	13.441	13.663	12.703
7.	13.435	13.611	13.435
8.	13.425	13.568	13.543
9.	13.314	13.127	13.650
10.	13.919	14.202	14.013
11.	13.774	13.824	13.820
12.	14.997	13.938	13.729
Average	13.544	13.613	13.635
Standard deviation	0.490	0.273	0,325

Table 12. Surface roughness Rz for VCMT inserts clamped in a collet chuck

Table 12 presents the measured surface roughness Rz values obtained using VCMT indexable inserts under the cutting conditions specified in Table 5 with workpieces clamped in a collet chuck. The reported Rz values represent the average of three measurements taken at 120° rotations at designated location A, B, or C.
Table 13 presents the measured surface roughness Ra values obtained using VCGT indexable inserts under the cutting conditions specified in Table 5 with workpieces clamped in a collet chuck. The reported Ra values represent the average of three measurements taken at 120° rotations at designated location A, B, or C.

	Mean value Ra, µm		
Sample	Location A	Location B	Location C
1.	3.007	3.395	3.069
2.	2.644	2.996	2.984
3.	2.951	3.024	3.008
4.	2.883	3.003	2.824
5.	3.289	3.304	3.335
6.	3.078	3.141	3.056
7.	3.019	3.025	3.098
8.	3.365	3.387	3.358
9.	3.375	3.409	3.447
10.	3.435	3.433	3.454
11.	3.480	3.496	3.538
12.	3.568	3.606	3.633
Average	3.175	3.268	3.234
Standard deviation	0.271	0.209	0.247

Table 13. Surface roughness Ra for VCGT inserts clamped in a collet chuck

The measured surface roughness parameters Rz of workpieces clamped in a collet chuck and machined with VCGT indexable inserts under the conditions listed in Table 5 are given in Table 14. Each listed Rz value is the mean of three measurements conducted with a 120° rotation at location A, B, or C.

	Mean value Rz, µm		
Sample	Location A	Location B	Location C
1.	12.677	13.140	13.225
2.	12.784	12.918	13.091
3.	12.490	12.755	12.811
4.	12.686	12.827	12.637
5.	13.572	13.650	14.023
6.	13.653	14.105	13.866
7.	13.383	13.487	14.261
8.	14.827	14.641	14.693
9.	14.510	14.758	14.984
10.	15.029	15.030	15.245
11.	15.128	15.415	15.768
12.	15.310	15.680	15.592
Average	13.837	14.034	14.183
Standard deviation	1.024	1.004	1.043

Table 14. Surface roughness Rz for VCGT inserts clamped in a collet chuck

Based on the results presented in Tables 7–14, a plot comparing the mean surface roughness Ra values along the evaluated section as a function of the workpiece clamping method and indexable insert type was constructed, as shown in Fig. 7.

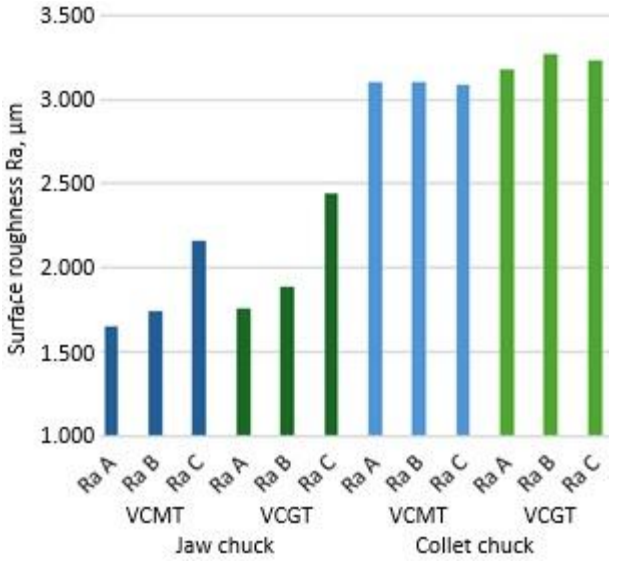


Figure 7. Comparison of mean surface roughness Ra of the machined surface for different clamping methods

Fig. 8 presents a comparison of the surface roughness Rz as a function of the workpiece clamping method and indexable insert type, constructed based on the results given in Tables 7–14. As shown by the graphical representation of the results in Figs. 7 and 8, the measured surface roughness values Ra and Rz exhibit a more uniform trend when using the collet chuck. When using the conventional three-jaw chuck, it is noticeable that the surface roughness Ra and Rz increases with increasing distance from the chuck toward the free end of the workpiece (see locations A, B, and C in Fig. 6). This effect can be attributed to low workpiece clamping rigidity and greater blank deflection caused by cutting forces. Additionally, an increase in the surface roughness of the components is observed when using VCGT indexable inserts, confirming the conclusions of Sorbino [2025].

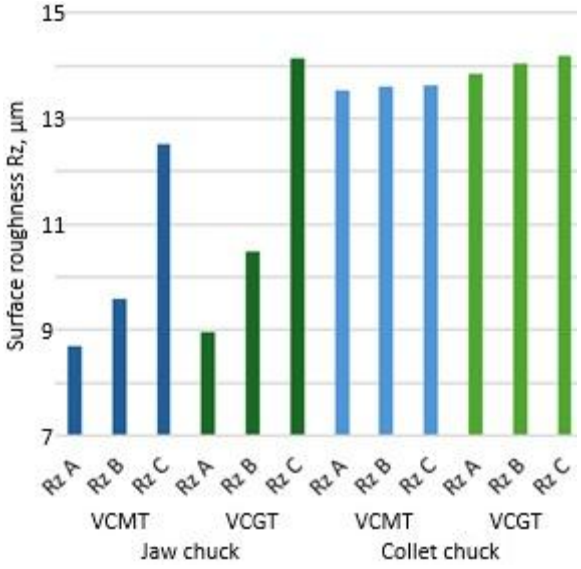


Figure 8. Comparison of mean surface roughness Rz of the machined surface for different clamping methods

The stability of the cutting process can be evaluated based on the standard deviation of individual measured values relative to the mean roughness. The standard deviation evaluation for individual measurements is presented in Table 15. As indicated by the data listed, collet chuck clamping resulted in a lower standard deviation. Although the surface roughness of workpieces clamped in the collet chuck increased under the cutting conditions given in Table 5, the surface topography

remains uniform along the full length of the part, as shown in Figs. 8 and 9 and confirmed by the standard deviations in Table 15. Lower surface roughness can be attained by optimizing the cutting parameters, which will be adjusted in actual production. From the standpoint of cutting process stabilization, this roughness increase (which remains strictly within the tolerances prescribed by technical documentation) is irrelevant to the scope of these experiments.

Chucking method	Cutting insert	Grand mean of roughness	Overall standard deviation σ
Jaw chuck	VCMT	Ra = 1.853 µm	0.278 µm
	VCMT	Rz = 10.272 µm	1.913 µm
	VCGT	Ra = 2.031 µm	0.338 µm
	VCGT	Rz = 11.189 µm	2.460 µm
Collet chuck	VCMT	Ra = 3.098 µm	0.068 µm
	VCMT	Rz = 13.597 µm	0.377 µm
	VCGT	Ra = 3.225 µm	0.247 µm
	VCGT	Rz = 14.018 µm	1.033 µm

Table 15. Evaluation of the standard deviation σ

4 CONCLUSIONS

This study addresses cutting process stabilization during turning using collet chuck clamping compared to conventional three-jaw chuck clamping. Tests were conducted with VCGT and VCMT indexable inserts when machining AISI 304 austenitic stainless steel. Based on the experimental results under specified cutting conditions, taking surface roughness parameters Ra and Rz alongside the standard deviation from the mean as evaluation criteria, collet chuck clamping provides greater cutting stability than a conventional chuck. Additionally, comparing VCMT and VCGT inserts showed that lower surface roughness is consistently obtained using VCMT inserts.

Based on the obtained results and their replication, it is possible to formulate specific conclusions that can be interpreted as potential advantages regarding the application of collet chucks:

a) using collet chucks enhances workpiece clamping stiffness and reduces bending compliance;

b) using collet chucks minimizes workpiece deflection under high cutting forces at the unsupported free end;

c) using collet chucks stabilizes the cutting operation and ensures a more uniform surface roughness profile along the component;

d) using collet chucks decreases overall production time by eliminating auxiliary non-productive times associated with tailstock clamping.

These results provide a foundation for future research into the machining of austenitic stainless steels and the surface integrity optimization of machined parts.

At the same time, they expand the knowledge base in the field of metalworking, which is part of technically oriented subjects taught at all levels of education.

ACKNOWLEDGMENTS

Supported by the project GFD_PdF_2025_001 Comparison of the conceptual analysis of the solved learning tasks and the quantitative analysis of the achieved level of pupils' knowledge in the context of STEM education and teaching.

The authors would like to thank the company TMC CR, s.r.o. for providing experimental material and advice on implementing the technology.

REFERENCES

[Anh 2025] Anh, N.T. and Tung, T.T. Methodical approach to fixture design in the milling of thin-walled mechanical components. Results in Engineering, 2025, Vol. 27, Art. No. 106518. DOI: 10.1016/j.rineng.2025.106518

[Botak 2024] Botak, Z., et al. Determination of Optimal Machining Parameters Based on Roughness and Vibration Measurements of Pieces Produced by Whirling on a Lathe Machine. Machines, 2024, Vol. 12, No. 5, Art. No. 328. DOI: 10.3390/machines12050328

[Boucherit 2021] Boucherit, S., et al. Modeling and optimization of cutting parameters during machining of austenitic stainless steel AISI304 using RSM and desirability approach. Periodica Polytechnica Mechanical Engineering, 2021, Vol. 65, No. 1, pp 10-26. DOI: 10.3311/PPme.12241

[Bratan 2023] Bratan, S., et al. New Calculation Methodology of the Operations Number of Cold Rolling Rolls Fine Grinding. Applied Sciences, 2023, Vol. 13, No. 6, 3484. DOI: 10.3390/app13063484

[Chinchanikar 2023] Chinchanikar, S. and Gadge, M. Performance modeling and multi-objective optimization during turning AISI 304 stainless steel using coated and coated-microblasted tools. Obrabotka Metallov, 2023, Vol. 22, No. 4, pp. 117-135. DOI: 10.17212/1994-6309-2023-25.4-117-135

[Coranic 2023] Coranic, T. and Mascenik, J. Experimental Measurement of Dynamic Characteristics of Structural Units. Processes, 2023, Vol. 11, No. 12, 3333. DOI: 10.3390/pr11123333

[Cubonova 2019] Cubonova, N., Dodok, T., Sagova, Z. Optimisation of the Machining Process using Genetic Algorithm. Scientific Journal of Silesian University of Technology-Series Transport, 2019, Vol. 104. DOI: 10.20858/sjsutst.2019.104.2

[Dua 2025] Dua, T.V., et al. Multi-Objective Optimization of the Turning Process using the Probability Method. Engineering, Technology and Applied Science Research, 2025, Vol. 15, No. 1, pp. 19865-19870. DOI: 10.48084/etasr.9472

[Feng 2022] Feng, Q., et al. Optimization of a clamping concept based on machine learning. Production Engineering, 2022, Vol. 16, No. 1, pp. 9-22. DOI: 10.1007/s11740-021-01073-z

[Feng 2025] Feng, J., et al. Research on the Layout Design of Auxiliary Support Modules for Suppressing Machining Chatter in Thin-Walled Beams. Materials, 2025, Vol. 18, No. 9, Art. No. 1986. DOI: 10.3390/ma18091986

[Heras 2020] Heras, E.S., et al. Automatic expanding mandrel with air sensing device: Design and analysis. Applied Sciences, 2020, Vol. 10, No. 7, Art. No. 2551. DOI: 10.3390/app10072551

[Hrehova 2016] Hrehova, S. Predictive Model to Evaluation Quality of the Manufacturing Process Using Matlab Tools. Procedia Engineering, 2016, Vol. 149, pp. 149-154. DOI: 10.1016/j.proeng.2016.06.649

[Mane 2025a] Mane, S., et al. Analysis of the Surface Quality Characteristics in Hard Turning Under a Minimal Cutting Fluid Environment. Applied Mechanics, 2025, Vol. 6, No. 1, Art. No. 5. DOI: 10.3390/applmech6010005

[Mathivanan 2021] Mathivanan, A., et al. Finite element simulation and regression modeling of machining

attributes on turning AISI 304 stainless steel. Manufacturing Review, 2021, Vol. 8, Art. No. 2021022. DOI: 10.1051/mfreview/2021022

[Mitursk a 2020] Mitursk a, I., et al. Development of a specialized lathe chuck for turning operations of cast iron rope wheels. Manufacturing Technology, 2020, Vol. 20, No. 2, pp. 210-216. DOI: 10.21062/MFT.2020.026

[Molnar 2023] Molnar, V., Influence of Cutting Parameters and Tool Geometry on Topography of Hard Turned Surfaces. Machines, 2023, Vol. 11, No. 6, Art. No. 665. DOI: 10.3390/machines11060665

[Olejarova 2021] Olejarova, S. and Krenicky, T. Influence of Vibration Magnitude in Machining of Materials by Turning Technology. MM Science Journal, 2021, Vol. October, pp. 4886-4890.

[Qtto 2015] Qtto, A., Khasawneh, F.A., Radons, G. Position-dependent stability analysis of turning with tool and workpiece compliance. International J. of Advanced Manufacturing Technology, 2015, Vol. 79, No. 9-12, pp. 1453-1463. DOI: 10.1007/s00170-015-6929-1

[Prydalnyi 2026] Prydalnyi, B., et al. Determining an Analytical Criterion for the Effective Speed of a Spindle Unit for the Automatic Machining of Long Workpieces. Eastern-European Journal of Enterprise Technologies, 2026, Vol. 3, No. 1, pp. 64-72. DOI: 10.15587/1729-4061.2026.362733

[Qin 2025] Qin, Z., et al. Chatter stability prediction methods in the machining processes: a review. International J. of Advanced Manufacturing Technology, 2025, Vol. 136, No. 7, pp. 2945-2985. DOI: 10.1007/s00170-024-14971-0

[Sakamoto 2012] Sakamoto, H., Matsuda, T. and Shimizu, S. Effect of clamped toolholders on dynamic characteristics of spindle system of machining center. International Journal of Automation Technology, 2012, Vol. 6, No. 2, pp. 168-174. DOI: 10.20965/ijat.2012.p0168

[Sorbino 2025] Sorbino, D.R.D., et al. Suitability of Vcgt and Vcmt Cutting Inserts Type for Turning Alsi 304 Steel. MM Science J., 2025, No. December, pp. 9020-9025. DOI: 10.17973/MMSJ.2025_12_2025103

[Ugras 2025] Ugras, R.C. and Altintas, Y. Optimization of clamping conditions in thin-walled part machining to minimize forced vibrations, Part I: Model for the single tool –workpiece contact location. CIRP Journal of Manufacturing Science and Technology, 2025, Vol. 61, pp. 103-113. DOI: 10.1016/j.cirpj.2025.05.015

[Zhang 2022] Zhang, Y., et al. Effects of Multi-Pass Turning on Stress Corrosion Cracking of AISI 304 Austenitic Stainless Steel. Applied Micromachines, 2022, Vol. 13, No. 10., Art. No. 1745. DOI: 10.3390/mi13101745

CONTACTS:

Ing. Jan Majernik, PhD.
University of South Bohemia in Ceske Budejovice
Faculty of Agriculture and Technology
Studentská 1668, 370 05 Ceske Budejovice. Czech Republic
jmajernik@jcu.cz

LICENSE CREATIVE COMMONS:

The article is published under the terms and conditions of the Creative Commons Attribution 4.0 International License (CC BY 4.0).